A Highly Reactive Ruthenium Phosphido Complex Exhibiting Ru−P π-Bonding

Eric J. Derrah,[†] Dimitrios A. Pantazis,[‡] Robert McDonald,[§] and Lisa Rosenberg*[,†]

Department of Chemistry, University of Victoria, P.O. Box 3065, Victoria, British Columbia V8W 3V6, Canada, WestCHEM, Department of Chemistry, University of Glasgow, Glasgow G12 8QQ, United Kingdom, and X-ray Crystallography Laboratory, Department of Chemistry, University of Alberta, Edmonton, Alberta T6G 2G2, Canada

Received January 3, 2007

Multiple bonding in the terminal phosphido complex [Ru(PCy_2)(η^5-indenyl)(PPh_3)] (**2a**) is clearly demonstrated by solution, solid-state, and computational studies. Reactions of this dark blue, half-sandwich complex with CO, MeI, $HNEt_3Cl$, HCl, NH_4PF_6, H_2, and Et_3SiH demonstrate an unusual range of behavior resulting from combined coordinative unsaturation at Ru, high nucleophilicity/basicity of the phosphido P, and π-character of the Ru−P interaction. The terminal, π-bound phosphido structure is general for a range of PR_2 species (R = Pr^i (**2b**), Ph (**2c**), Tol^p (**2d**)). The very reactive diarylphosphido analogues **2c**,**d** have been observed spectroscopically at low temperatures and can be trapped quantitatively as their CO adducts, [Ru(PAr_2)(η^5-indenyl)(CO)(PPh_3)] (**3c**,**d**), in which the Ru−P bond order is reduced to 1. Complex **2a** and its analogue [Ru(PPr^i_2)(η^5-indenyl)(PPh_3)] (**2b**) are consistently isolated with ∼15% of their structural isomers, the ruthenium hydrido phosphaalkenes **9a**,**b**, resulting from an apparent 1,2-H shift.

Introduction

Phosphido ligands are best known in ruthenium chemistry and elsewhere as exemplary bridging ligands (μ-PR_2) in dinuclear complexes or larger clusters.[1] The few reported examples of terminal Ru−PR_2 complexes are formally 6-coordinate, 18-electron complexes, with pyramidal geometry at phosphorus indicative of a stereoactive lone pair and Ru−PR_2 distances consistent with a Ru−P single bond.[2] Examples in which the lone pair on phosphorus participates in π-bonding with the metal center are unknown for ruthenium and indeed remain rare for groups 8−10.[3] This mode of binding, which leads to planarity at an sp^2-hybridized phosphorus and a shortened M−P distance, is not uncommon for early-metal complexes (groups 4−7),[4] where it represents an alternative to dimerization (via μ-PR_2) to offset electron deficiency and coordinative unsaturation. Thus, complexes that are formally 16-electron species if the phosphido ligand participates only in σ-bonding (1-electron donor) achieve an 18-electron count through the additional formation of a metal−phosphorus π-bond (3-electron donor).[5] We report herein the first fully characterized example of a ruthenium−phosphorus double bond,[6] observed for an "unsaturated", two-legged piano-stool complex.

Results and Discussion

Experimental and Computational Characterization of the π-Bond in [Ru(PCy_2)(η^5-indenyl)(PPh_3)] (2a). The mixed phosphine complex [RuCl(η^5-indenyl)($HPCy_2$)(PPh_3)] (**1a**)[7] is quantitatively consumed by addition of $KOBu^t$, with loss of KCl and Bu^tOH. The resulting dark blue complex [Ru(PCy_2)(η^5-indenyl)(PPh_3)] (**2a**) (Scheme 1) is invariably accompanied by a small amount of the metallaphosphaalkene hydride complex [Ru(P{=C(−C_5H_{10}−)}Cy)(H)(η^5-indenyl)(PPh_3)] (**9a**), a struc-

* To whom correspondence should be addressed. E-mail: lisarose@uvic.ca.
† University of Victoria.
‡ University of Glasgow.
§ University of Alberta.

(1) Carty, A. J.; MacLaughlin, S. A.; Nucciarone, D. *Methods Stereochem. Anal.* **1987**, *8*, 559.

(2) (a) Planas, J. G.; Hampel, F.; Gladysz, J. A. *Chem. Eur. J.* **2005**, *11*, 1402. Planas, J. G.; Gladysz, J. A. *Inorg. Chem.* **2002**, *41*, 6947. (b) Sterenberg, B. T.; Udachin, K. A.; Carty, A. J. *Organometallics* **2003**, *22*, 3927. (c) Stasunik, A.; Wilson, D. R.; Malisch, W. *J. Organomet. Chem.* **1984**, *270*, C18. (d) Chan, V. S.; Stewart, I. C.; Bergman, R. G.; Toste, F. D. *J. Am. Chem. Soc.* **2006**, *128*, 2786. (e) Burn, M. J.; Fickes, M. G.; Hollander, F. J.; Bergman, R. G. *Organometallics* **1995**, *14*, 137. (f) Bohle, D. S.; Jones, T. C.; Rickard, C. E. F.; Roper, W. R. *Organometallics* **1986**, *5*, 1612. (g) Weber, L.; Reizig, K.; Boese, R. *Organometallics* **1985**, *4*, 2097.

(3) Metals from groups 8−10 for which crystallographically characterized π-bound phosphido complexes have been reported are limited to Co (Lang, H.; Eberle, U.; Leise, M.; Zsolnai, L. *J. Organomet. Chem.* **1996**, *519*, 137. Bezombes, J. P.; Hitchcock, P. B.; Lappert, M. F.; Nycz, J. E. *Dalton Trans.* **2004**, 499) and Ni (Melenkivitz, R.; Mindiola, D. J.; Hillhouse, G. L. *J. Am. Chem. Soc.* **2002**, *124*, 3846).

(4) Examples of π-bound phosphido complexes of metals from groups 4−7 include: (a) Baker, R. T.; Calabrese, J. C.; Harlow, R. L.; Williams, I. D. *Organometallics* **1993**, *12*, 830. (b) Baker, R. T.; Calabrese, J. C.; Glassman, T. E. *Organometallics* **1988**, *7*, 1889. (c) Cowley, A. H.; Kemp, R. A. *Chem. Rev.* **1985**, *85*, 367. (d) Cowley, A. H.; Giolando, D. M.; Nunn, C. M.; Pakulski, M.; Westmoreland, D.; Norman, N. C. *J. Chem. Soc., Dalton Trans.* **1988**, 2127. (e) Lang, H.; Leise, M. Zsolnai, L. *J. Organomet. Chem.* **1990**, *389*, 325. (f) Malisch, W.; Hirth, U. A.; Bright, T. A.; Kab, H.; Ertel, T. S.; Huckmann, S.; Bertagnolli, H. *Angew. Chem., Int. Ed. Engl.* **1992**, *31*, 1525. (g) Malisch, W.; Hirth, U. A.; Grun, K.; Schmeusser, M. *J. Organomet. Chem.* **1999**, *572*, 207.

(5) π-Bound phosphido (PR_2^-) complexes (nucleophilic at P, three-electron-donor ligands) are distinct from phosphenium (PR_2^+) complexes (electrophilic at P, two-electron-donor ligands), which may also exhibit π-bonding to metals by virtue of their π-acidity. See: (a) Sanchez, M.; Mazières, M. R.; Lamadé, L.; Wolf, R. In *Multiple Bonds and Low Coordination in Phosphorus Chemistry*; Regitz, M., Scherer, O. J., Eds.; Georg Thieme Verlag: Stuttgart, Germany, 1990; p 141. (b) Abrams, M. B.; Scott, B. L.; Baker, R. T. *Organometallics* **2000**, *19*, 4944. (c) Nakazawa, H. *J. Organomet. Chem.* **2000**, *611*, 349.

(6) A series of metastable Ru−phosphenium complexes exhibit ^{31}P NMR shifts consistent with sp^2 planar phosphorus, but the extent of π-back-bonding from Ru has not been assessed: Kawamura, K.; Nakazawa, H.; Miyoshi, K. *Organometallics* **1999**, *18*, 4785.

(7) Derrah, E. J.; Marlinga, J. C.; Mitra, D.; Friesen, D. M.; Hall, S. A.; McDonald, R.; Rosenberg, L. *Organometallics* **2005**, *24*, 5817.

10.1021/om0700056 CCC: $37.00
Publication on Web 02/16/2007

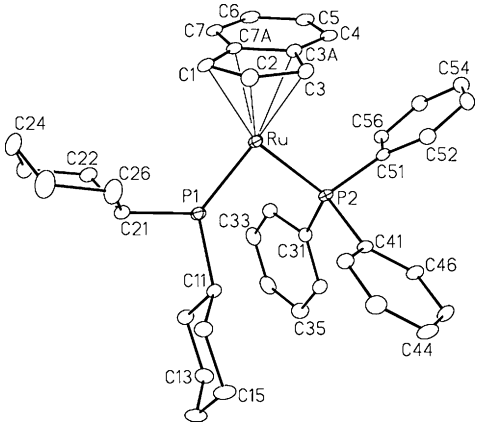

Figure 1. View of [Ru(PCy_2)(η^5-indenyl)(PPh_3)] (**2a**) without hydrogen atoms. In this and subsequent figures, non-hydrogen atoms are represented by Gaussian ellipsoids at the 20% probability level, C* denotes the centroid of the plane defined by C(7A)−C(1)−C(2)−C(3)−C(3A), and Δ (indenyl slip distortion) = *d*[Ru−C(7A),C(3A)] − *d*[Ru−C(1),C(3)]. Selected interatomic distances (Å) and bond angles (deg): Ru−P(1) = 2.1589(14), Ru−P(2) = 2.2719(12), Ru−C* = 1.885, Δ = 0.117; P(1)−Ru−P(2) = 92.62-(5), P(1)−Ru−C* 138.4, P(2)−Ru−C* = 128.4, Ru−P(1)−C(11) = 129.54(17), Ru−P(1)−C(21) = 125.44(17), C(11)−P(1)−C(21) = 103.2(2).

Scheme 1

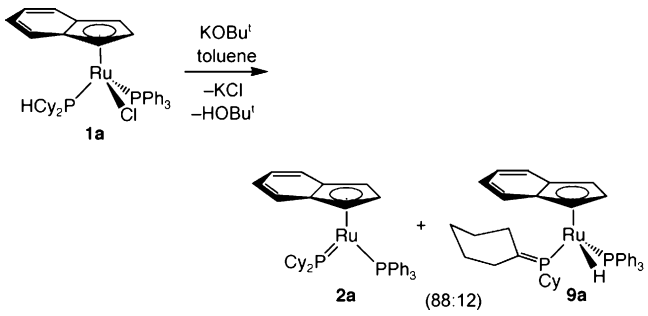

tural isomer that appears to be in equilibrium with **2a** and is consumed on reaction with small molecules (vide infra). Solution NMR and X-ray crystallographic studies indicate that the major product **2a** is best viewed structurally as containing a double bond between PCy_2 and Ru, with the phosphido ligand behaving as a three-electron donor. The $^{31}P\{^1H\}$ NMR spectrum for **2a** in d_6-benzene shows the expected doublet for PPh_3 at 63.4 ppm ($^2J_{PP}$ = 65 Hz), but the corresponding doublet for PCy_2 is at 276.3 ppm, an extreme downfield shift typical of planar "sp^2" phosphorus.[4a,d,8,9] $\delta(HPCy_2)$ for **1a** is 68.3 ppm. The molecular structure of **2a** (Figure 1) shows the sum of angles at the phosphido P to be 358.2°, indicating the planarity at P consistent with π-bonding.

DFT calculations clearly reproduce the planarity of the phosphido ligand observed crystallographically. The calculated Ru−PPh_3 and Ru−PCy_2 distances also agree well with the solid-state structure of **2a**: 2.266 and 2.166 Å, respectively, compared with 2.2719(12) and 2.1589(14) Å for the crystal structure. The

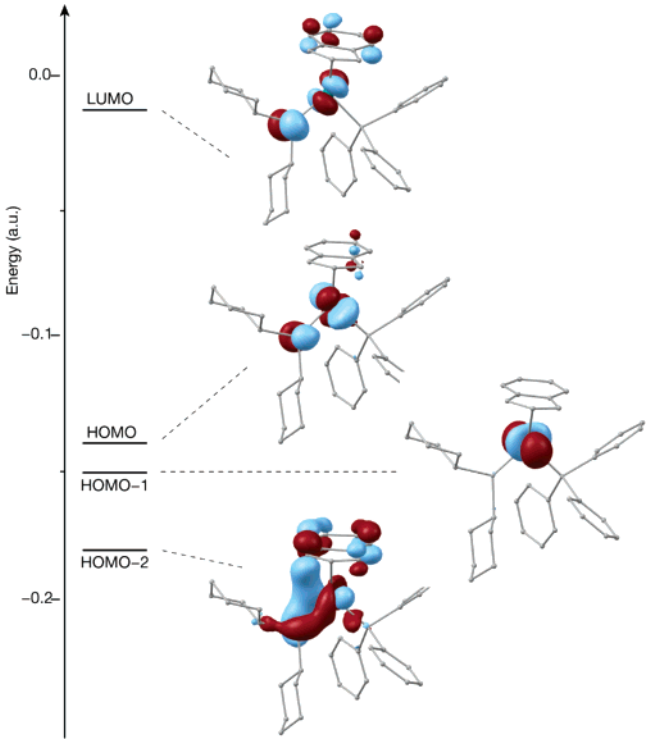

Figure 2. Frontier Kohn−Sham molecular orbitals calculated using DFT (hybrid PBE1PBE) for [Ru(η^5-indenyl)(PCy_2)(PPh_3)] (**2a**).

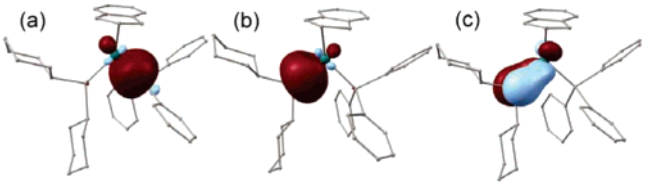

Figure 3. Occupied natural orbitals relevant to Ru−P bonds resulting from NBO analysis of the calculated structure of **2a**: (a) Ru−PPh_3 σ; (b) Ru−PCy_2 σ; (c) Ru−PCy_2 π.

frontier Kohn−Sham molecular orbitals (Figure 2) show a distribution of the π-character of the ruthenium phosphide over three valence orbitals: HOMO-2, HOMO, and LUMO. In contrast, HOMO-1 is purely Ru-based, a 4d orbital with lobes protruding perpendicularly on either side of the RuP_2 plane. Within the π-manifold, HOMO-2 corresponds to the Ru−P π-bonding combination, with strong mixing with an indenyl-based orbital, while the unoccupied π-antibonding component defines the LUMO of the system.

To firmly establish the Ru−PCy_2 bond order, we analyzed these calculations using several different methods. An unequivocal picture of the bonding in **2a** emerges from natural bond orbital (NBO) analysis,[10a] which clearly identifies both a σ (sd/sp)- and a π (d/p)-bond between Ru and PCy_2, as well as a σ-bond between Ru and PPh_3 (Figure 3). Calculated bond ellipticities[10b] of 0.031 (Ru−PPh_3) and 0.162 (Ru−PCy_2) are also consistent with the significant π-character of the ruthenium−

(8) Hutchins, L. D.; Paine, R. T.; Campana, C. F. *J. Am. Chem. Soc.* **1980**, *102*, 4521.

(9) A downfield ^{31}P shift of 185.8 ppm was reported for a rhodium tris(phosphine) complex containing the PCy_2 ligand. Although this terminal phosphido complex was not structurally characterized, computational studies on the simple model $(H_3P)_3RhPH_2$ point to significant P (p)−Rh (p) π-interactions, leading to preferential stabilization of, and contribution of, a rotamer in which the P_3Rh and PH_2 fragments are entirely coplanar. Dahlenburg, L. Höck, N.; Berke, H. *Chem. Ber.* **1988**, *121*, 2083.

(10) (a) Reed, A. E.; Curtiss, L. A.; Weinhold, F. *Chem. Rev.* **1988**, *88*, 899. (b) The bond ellipticity parameter (ϵ) emerges from topological analysis of electron density associated with molecular bonds; it is a quantitative measure of the deviation of the electron distribution from cylindrical symmetry, i.e. of the amount of π-character of a bond. Benchmark ϵ values are 0.000 and 0.298 for the C−C bonds of ethane and ethylene, respectively. Bader, R. F. W. *Atoms in Molecules: A Quantum Theory*; Oxford University Press: Oxford, U.K., 1994. (c) Wiberg bond indices provide an indication of the relative bond order between specific atom pairs and are calculated on the basis of the orthonormal natural atomic orbitals produced by the NBO analysis. Wiberg, K. B. *Tetrahedron* **1968**, *24*, 1083.

Scheme 2

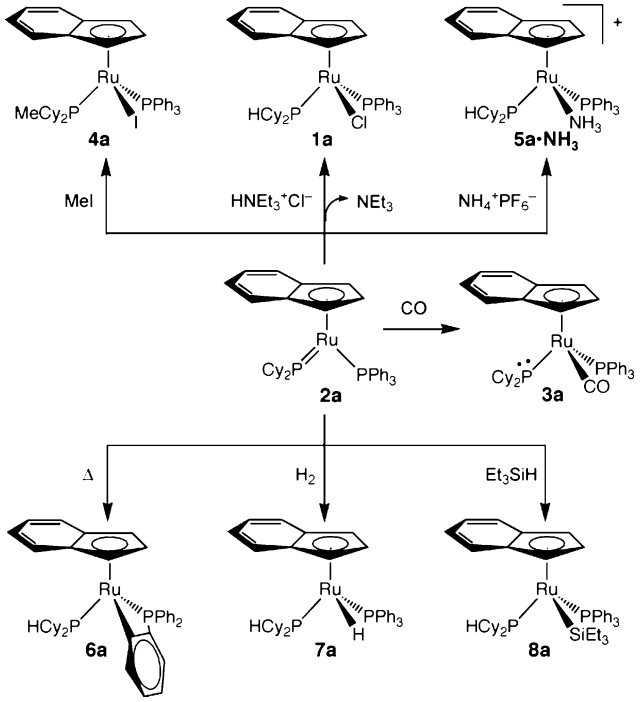

phosphido interaction. Finally, for Ru−PCy_2 the calculated Wiberg bond index,[10c] a relative measure of bond order, is exactly double that for Ru−PPh_3 (1.18 vs 0.59), confirming the presence of the Ru=P double bond.

The dark blue color of **2a** places it among an interesting and limited series of two-legged piano-stool ruthenium complexes.[11,12] Of these, **2a** is the first structurally characterized example containing either an η^5-indenyl ligand or a terminal phosphido ligand. These five-coordinate compounds are invariably planar at ruthenium (see Figure 1 for relevant angles) and typically include at least one X ligand (e.g., halide, alkoxide, amido, and thiolato ligands) with a lone pair able to interact in a π-fashion with the ruthenium. The extent of this π-bonding can vary considerably,[13] yet these intensely colored complexes all exhibit reactivity dominated by coordinative unsaturation at ruthenium (vide infra).[11] The UV spectrum of **2a** in either toluene or diethyl ether shows a band at 590 nm ($\epsilon = 1700$), which is responsible for its deep blue color. Time-dependent DFT calculations suggest this band corresponds largely to the HOMO−LUMO transition (n to π^*), for which there is no net transfer of charge. A second band at 370 nm ($\epsilon = 10\,000$) corresponds to the HOMO-2−LUMO transition (π to π^*), but again, charge transfer does not play a role.

Reactions of [Ru(PCy_2)(η^5-indenyl)(PPh_3)] (2a). Although **2a** is formally an 18-electron complex, it behaves as a coordinatively unsaturated analogue of the highly P-basic/nucleophilic ruthenium phosphido complexes reported recently by Gladysz and co-workers, [Ru(PR_2)(η^5-C_5H_5)(PR'_3)$_2$].[2a] Functional unsaturation at Ru is demonstrated by ready formation

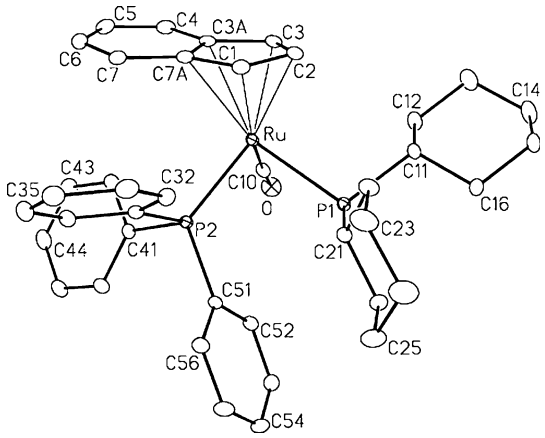

Figure 4. Molecular structure of [Ru(PCy_2)(η^5-indenyl)(CO)(PPh_3)] (**3a**). Selected interatomic distances (Å) and bond angles (deg): Ru−P(1) = 2.4390(7), Ru−P(2) = 2.3158(6), Ru−C* = 1.973, Δ = 0.154; P(1)−Ru−P(2) = 90.92(2), P(1)−Ru−C* = 125.8, P(2)−Ru−C* = 125.4, Ru−P(1)−C(11) = 107.36(8), Ru−P(1)−C(21) = 107.88(8), C(11)−P(1)−C(21) = 102.47(10).

of dark red [Ru(PCy_2)(η^5-indenyl)(CO)(PPh_3)] (**3a**) on addition of CO(g) to **2a** (Scheme 2 (middle) and Figure 4). Loss of the Ru−P π-bond in this transformation is strikingly demonstrated by an increase of almost 0.3 Å in the Ru−PCy_2 distance in **3a** relative to **2a** and by a ~200 ppm upfield shift of the ^{31}P peak for PCy_2 in **3a** relative to **2a**, consistent with a change from planar to tetrahedral geometry at the terminal phosphido ligand.[14]

The $Ru^{\delta+}$=$P^{\delta-}$ bond polarity is indicated by a series of reactions (Scheme 2 (top)), including that of **2a** with MeI, in which $Me^{\delta+}$ is delivered to the phosphido ligand and $I^{\delta-}$ coordinates to ruthenium, to generate [Ru(η^5-indenyl)(I)($MePCy_2$)(PPh_3)] (**4a**). The phosphido ligand in **2a** can also be protonated by $HNEt_3Cl$: this delivers Cl^- to the more electropositive, unsaturated ruthenium, regenerating orange **1a**. This reaction may proceed via the cationic triethylamine adduct [Ru(η^5-indenyl)($HPCy_2$)(NEt_3)(PPh_3)]$^+$ (**5a·NEt$_3$**). Structural evidence for this intermediate was obtained by adding NH_4PF_6 to **2a**, which allowed isolation of yellow crystals of the ammine complex [Ru(η^5-indenyl)($HPCy_2$)(NH_3)(PPh_3)]$^+$ (**5a·NH$_3$**) as its PF_6^- salt (Figure 5). Protonation of **2a** by ethereal HCl also gives **1a** as the major product, but an increase in the proportion of byproducts is observed, presumably reflecting the high reactivity of an unsaturated fragment of the formula [Ru(η^5-indenyl)($HPCy_2$)(PPh_3)]$^+$.[15]

Further evidence for the combined PCy_2 basicity and functional unsaturation of complex **2a** comes from its thermal (solution) transformation into ortho-metalated **6a** (Scheme 2 (bottom left)).[16] Also, while other examples of blue "unsaturated" ruthenium complexes are notable for their ability to coordinate η^2-H_2 or for their susceptibility to oxidative addition reactions leading to Ru(IV) complexes,[11] addition of H_2 or $HSiEt_3$ to **2a** leads instead to effective 1,2-addition across the

(11) Dark blue, black, or purple complexes of the formula [Ru(η^5-C_5Me_5)(X)(L)] are reviewed in: Jimenez-Tenorio, M.; Puerta, M. C.; Valerga, P. *Eur. J. Inorg. Chem.* **2004**, 17.

(12) Dark blue or black complexes of the formula [Ru(X)$_2$(η^6-arene)] include: (a) Mashima, K.; Kaneyoshi, H.; Kaneko, S.; Mikami, A.; Tani, K.; Nakamura, A. *Organometallics* **1997**, *16*, 1016. (b) Haack, K. J.; Hashiguchi, S.; Fujii, A.; Ikariya, T.; Noyori, R. *Angew. Chem., Int. Ed.* **1997**, *36*, 285.

(13) Dark blue Ru piano-stool complexes in which both "legs" are L-type ligands, and thus incapable of π-donation to Ru, have also recently been reported.[11]

(14) Very low $^2J_{PP}$ values in **3a** are also similar to those reported in ref 2a, for mixed PR_2/PR'_3 complexes of Ru. Similar shift and coupling constant changes were also observed for complexes **3c**,**d**.

(15) The high reactivity of [Ru(η^5-C_5R_5)(PR'_3)$_2$]$^+$ complexes is well-described in ref 11.

(16) The presence of ortho-metalated PPh_3 is diagnosed in **6a** by an upfield shift of 84 ppm for δ(^{31}P) relative to **2a**. Garrou, P. E. *Chem. Rev.* **1981**, *81*, 229. We have observed peaks due to the analogous decomposition product, **6b**, in NMR samples of **2b** that have sat at room temperature for several hours. $^{31}P\{^1H\}$ NMR (145.80 MHz, δ): 66.5 (d, J_{PP} = 28 Hz, HP^iPr$_2$), −20.8 (d, PPh_3).

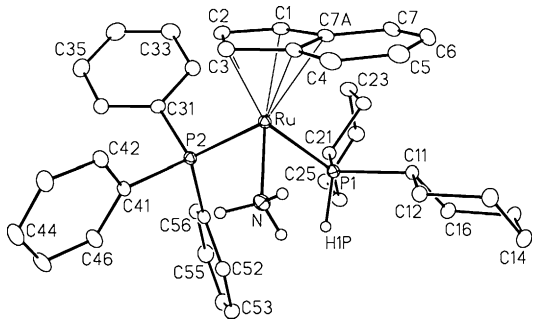

Figure 5. View of the complex cation **5a·NH$_3$**, [Ru(η^5-indenyl)(NH$_3$)(HPCy$_2$)(PPh$_3$)]$^+$. The hydrogen atoms attached to P(1) and N are shown with arbitrarily small thermal parameters; other hydrogen atoms are not shown. The hydrogen atom attached to P1 was located and freely refined. Selected interatomic distances (Å) and bond angles (deg): Ru−P(1) = 2.3309(5), Ru−P(2) = 2.2717(5), Ru−N = 2.1896(17), Ru−C* = 1.905, P(1)−H(1P) = 1.30(2), Δ = 0.134; P(1)−Ru−P(2) = 91.531(18), P(1)−Ru−N = 89.60(5), P(2)−Ru−N = 92.13(5), C*−Ru−P(1) = 127.2, C*−Ru−P(2) = 124.6, C*−Ru−N = 121.6.

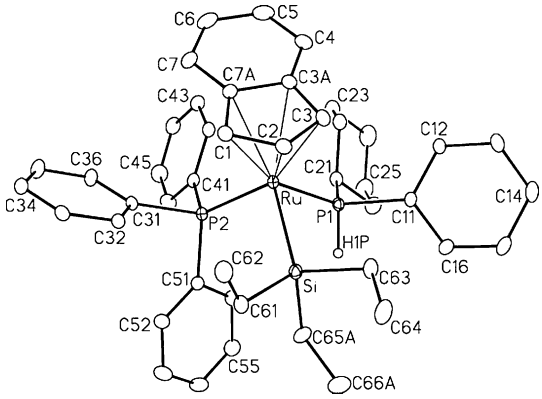

Figure 6. View of [Ru(η^5-indenyl)(SiEt$_3$)(HPCy$_2$)(PPh$_3$)] (**8a**). The phosphine hydrogen atom H(1P) (located and freely refined) is shown with an arbitrarily small thermal parameter; other hydrogen atoms are not shown. Selected interatomic distances (Å) and bond angles (deg): Ru−P(1) = 2.2790(7), Ru−P(2) = 2.2802(7), Ru−Si = 2.4108(8), Ru−C* = 1.965, P(1)−H(1P) = 1.32(3), Δ = 0.199; P(1)−Ru−P(2) = 96.05(3), P(1)−Ru−Si = 86.27(2), P2−Ru−Si = 96.19(2), C*−Ru−P(1) = 127.9, C*−Ru−P(2) = 125.0, C*−Ru−Si = 115.5.

Ru$^{\delta+}$=P$^{\delta-}$ double bond, to generate complexes **7a**[7] and **8a** (Figure 6), respectively (Scheme 2 (bottom right)).[17]

Computational and experimental studies are underway to probe whether these reactions rely on an equilibrium between **2a** and a 16-electron intermediate, where loss of the Ru−P π-bond gives a vacant coordination site at Ru and an extremely basic lone pair at now-pyramidal PR$_2$,[18] or on a concerted process initiated by nucleophilic attack of the PCy$_2$ group in **2a** at the hydrogen of each of these E−H bonds (E = Cl, C, H, Si). This behavior is also relevant in the context of base-promoted catalytic hydrophosphination by group 8 metals.[19] Cycloaddition reactions of the Ru=P double bond in **2a**−**d** with

Scheme 3

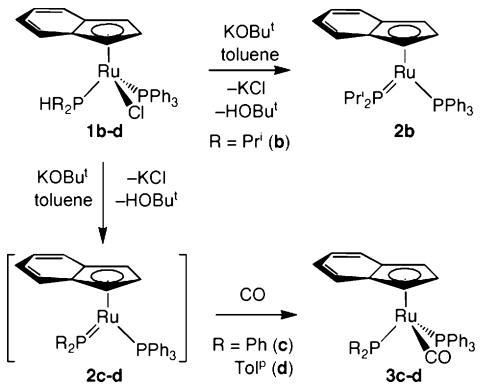

polar and nonpolar unsaturated organic fragments, leading to P−C bond formation,[20] are now underway and will be reported in due course.

Generality of Ru=PR$_2$ Bonding. The analogous terminal phosphido complex [Ru(PPr$^i_2$)(η^5-indenyl)(PPh$_3$)] (**2b**) is obtained when KOBu^t is added to the secondary phosphine complex **1b**,[21] which contains HPPr$^i_2$ (Scheme 3). The Ru−PPr$^i_2$ π-bond is readily diagnosed by ^{31}P{^{1}H} NMR, which shows a peak due to the phosphido ligand at the extreme downfield shift of 288.3 ppm. Unsurprisingly, when the bulky Cy and Pr^i groups in **2a**,**b** are replaced by aryl substituents, the resulting complexes **2c**,**d** (R = Ph (**c**), Tol^p (**d**)) are much more reactive. They have been observed by ^{31}P NMR spectroscopy at low temperature but decompose quickly at room temperature to a number of unidentified products. However, both of these complexes can be trapped quantitatively as their CO adducts **3c**,**d**[14] by addition of KOBu^t to **1c**[7] and **1d**[21] under an atmosphere of carbon monoxide. These reactions point to the ready formation of the terminal phosphido complexes and their fast reaction with available L-donor ligands.

Structural Isomerism at Ru-Bound sp^2 Phosphorus. Complex **2a** is invariably accompanied by a small amount of a hydride-containing species that we have identified as the metallaphosphaalkene complex [Ru(P{=C(−C$_5$H$_{10}$−)}Cy)(H)(η^5-indenyl)(PPh$_3$)] (**9a**) (Scheme 4). The structural isomerism of **2a** and **9a** is supported by mass spectrometric analysis of the mixture, and the continued presence of sp^2-hybridized phosphorus in **9a** is indicated by a signal at 243.3 ppm in the ^{31}P{^{1}H} NMR spectrum. Likewise, complex **2b** is consistently accompanied by ∼16% of the structural isomer [Ru(P{=C(CH$_3$)$_2$}Pr^i)(H)(η^5-indenyl)(PPh$_3$)] (**9b**) (δ(^{31}P) 256.4 ppm). As shown in Figure 7, signals in the alkyl region of the ^{1}H and ^{1}H{^{31}P} NMR spectra are particularly diagnostic of the phosphaalkene structure of **9b**, as confirmed by COSY and ^{1}H/^{13}C HSQC and HMBC experiments. Two sets of signals are observed for diastereotopic Pr^i groups in the major isomer **2b**,

(17) Similar reactions of H$_2$(g) were observed previously at nucleophilic terminal phosphido complexes of Ir (Fryzuk, M. D.; Bhangu, K. *J. Am. Chem. Soc.* **1988**, *110*, 961) and Rh.[9]

(18) Spectroscopic evidence for an equilibrium between the pyramidal phosphido complex [OsCl(PHPh)(CO)$_2$(PPh$_3$)$_2$] and an isomer exhibiting planar binding at phosphorus, [Os(PHPh)(CO)$_2$(PPh$_3$)$_2$]$^+$Cl$^-$, has been reported; however, this putative cationic intermediate exhibits umpolung at P, behaving formally as an electrophilic PHPh$^+$ complex. Bohle, D. S.; Jones, T. C.; Rickard, C. E. F.; Roper, W. R. *J. Chem. Soc., Chem. Commun.* **1984**, 865.

(19) (a) Jerome, F.; Monnier, F.; Lawicka, H.; Derien, S.; Dixneuf, P. H. *Chem. Commun.* **2003**, 696. (b) Malisch, W.; Klupfel, B.; Schumacher, D.; Nieger, M. J. *Organomet. Chem.* **2002**, *661*, 95. (c) Wicht, D. K.; Glueck, D. S. In *Catalytic Heterofunctionalization*; Togni, A., Gruetzmacher H. J., Eds.; Wiley-VCH: Weinheim, Germany, 2000; pp 143−170.

(20) A range of cycloaddition reactions at π-bound phosphido ligands on W and Mo have been reported by Malisch et al. See for example: (a) Malisch, W.; Grun, K.; Fey, O.; El Baky, C. A. *J. Organomet. Chem.* **2000**, *595*, 285. (b) Malisch, W.; El Baky, C. A.; Grun, K.; Reising, J. *Eur. J. Inorg. Chem.* **1998**, 1945. (c) Malisch, W.; Grun, K.; Fried, A.; Reich, W.; Pfister, H.; Hutter, G.; Zsolnai, L. *J. Organomet. Chem.* **1998**, *566*, 271. (d) Malisch, W.; Hahner, C.; Grun, K.; Reising, J.; Goddard, R.; Kruger, C. *Inorg. Chim. Acta* **1996**, *244*, 147.

(21) Data for **1b** are as follows. ^{31}P{^{1}H} NMR (145.79 MHz, δ): 75.9 (d, J_{PP} = 44 Hz, *P*^{i}Pr$_2$), 51.0 (d, *P*Ph$_3$). Data for **1d** are as follows. ^{31}P{^{1}H} NMR (145.79 MHz, δ): 49.8 (d, J_{PP} = 49 Hz, *P*Tol$^p_2$), 47.4 (d, *P*Ph$_3$).

Scheme 4

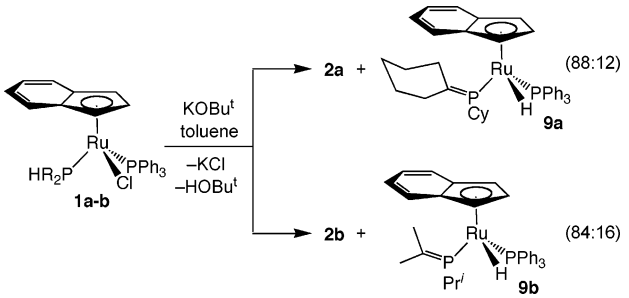

while the smaller peaks due to **9b** show that both the Pr^i methyl groups and the P═C$(CH_3)_2$ methyl groups in this minor isomer are diastereotopic.

The isomer ratios of **2a**/**9a** and **2b**/**9b**, determined by solution $^{31}P\{^1H\}$ NMR spectroscopy, are consistent over a range of crude and recrystallized samples, which suggests that the two complexes are in equilibrium. However, VT-NMR studies and ^1H and ^{31}P EXSY experiments for **2a**/**9a** provide no evidence for this equilibrium in solution on the NMR time scale. The relative amount of **9b** drops to 14% in the low-temperature $^{31}P\{^1H\}$ NMR spectrum of **2b**/**9b** in d_8-toluene, and ^1H EXSY on this mixture at room temperature shows very low intensity correlation between the Pr^i-derived methyl signals for the two isomers, but these results are not significant within experimental error. Consistent with slow conversion between isomers **2** and **9** in solution on the NMR time scale, DFT calculations on the simplified model complexes [RuCp(PHMe)(PH_3)] and [RuCp(H)-$(PHCH_2)(PH_3)$] show the hydrido isomer to be 9.8 kcal/mol higher in energy, which roughly accounts for the smaller observed amount of **9**, and give a transition state connecting the two species for which the barrier from [RuCp(PHMe)(PH_3)] is 60.7 kcal/mol. We continue to probe the mechanism of formation and/or exchange of these isomers, which may derive from base-catalyzed (i.e., occurring during the synthesis of **2**, in the presence of OBu^{t-}) or photolytically induced 1,2-H-shifts. We presume that purified **2** and **9** are in equilibrium but exchange relatively slowly in solution and that the consistent isomer ratios observed following various reaction/precipitation procedures suggest that the two isomers have remarkably similar solubilities.

Conclusion

We have prepared a series of coordinatively unsaturated, terminal phosphido complexes of ruthenium in which the presence of a Ru−P double bond provides interesting new pathways of reactivity. These complexes are of interest not only as models for intermediates in hydrophosphination but also in the context of Ru-mediated catalysis in general (e.g., transfer hydrogenation, olefin metathesis, olefin cyclopropanation), given the importance of, and analogy to, other Ru−ligand multiple bonds (Ru═N, Ru═C).

Experimental Section

General Considerations. Unless otherwise noted, all reactions and manipulations were performed under nitrogen in an MBraun Unilab 1200/780 glovebox or using conventional Schlenk techniques. All solvents were sparged with nitrogen for 25 min and dried using an MBraun Solvent Purification System (SPS). Deuterated solvents were purchased from Canadian Isotope Labs (CIL), freeze−pump−thaw-degassed, and vacuum-transferred from sodium/benzophenone (d_6-benzene, d_8-toluene) or calcium hydride (d-chloroform, d_2-dichloromethane) before use. Potassium *tert*-butoxide, ammonium hexafluorophosphate, triethylamine hydrochloride, triethylsilane and 2 M ethereal hydrogen chloride were purchased from Aldrich Chemical Co. and used as received without further purification. Carbon monoxide and hydrogen gas were purchased from Praxair Canada Inc.; hydrogen gas was passed through a drying/deoxygenating column containing activated molecular sieves (4 Å) and copper beads prior to use. [Ru(η^5-indenyl)-Cl$(HPR_2)(PPh_3)_2$] (**1a** (R = Cy), **1c** (R = Ph)) were prepared as previously reported in the literature;[7] complexes **1b** (R = Pr^i) and **1d** (R = Tol^p) were prepared with 90−95% purity using the same method[21] and were used without further purification. (All secondary phosphines were purchased from Strem Chemicals as 10 wt % solutions in hexanes (concentrations checked against a known quantity of triphenylphosphine oxide by $^{31}P\{^1H\}$ NMR before use), except for di-*p*-tolylphosphine, which was purchased neat.) NMR spectra were recorded on a Bruker Avance 500 instrument operating at 500.13 MHz for ^1H, 125.77 MHz for ^{13}C, 202.46 MHz for ^{31}P, and 99.36 MHz for ^{29}Si or on a Bruker Avance 360 operating at 145.80 MHz for ^{31}P. Unless otherwise noted, chemical shifts are reported in ppm at ambient temperature. ^1H chemical shifts are referenced to residual protonated solvent peaks at 7.16 (C_6D_5H), 2.09 ($PhCD_2H$), 7.24 ($CHCl_3$), and 5.32 ppm ($CDHCl_2$). ^{13}C chemical shifts are referenced to C_6D_6 at 128.4 ppm, $CDCl_3$ at 77.5 ppm, and CD_2Cl_2 at 54.0 ppm. All ^1H, ^{13}C, and ^{29}Si chemical shifts are reported relative to tetramethylsilane, and ^{31}P chemical shifts are reported relative to 85% H_3PO_4(aq). Microanalysis was performed by Canadian Microanalytical Service Ltd., Delta, BC, Canada. Melting/decomposition temperatures are uncorrected for ambient pressure. Inert-atmosphere MALDI-MS was carried out by Prof. Deryn E. Fogg and Johanna Blacquiere, Department of Chemistry, University of Ottawa.

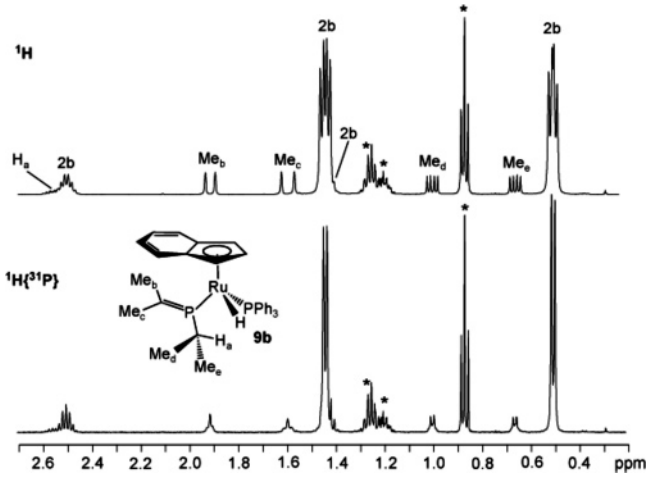

Figure 7. 500.13 MHz ^1H and $^1H\{^{31}P\}$ NMR spectra of an 84:16 mixture of **2b** and **9b** in d_6-benzene (asterisks indicate signals due to pentane, with which the complex mixture cocrystallizes).

^1H and $^{13}C\{^1H\}$ NMR data are given in Tables 1 and 2, and crystal data are given in Table 3.

Preparative-Scale Reactions.

(a) [Ru$(PCy_2)(\eta^5$-indenyl$)(PPh_3)$] (2a). Method A. To a dark red solution/suspension of **1a** (500 mg, 0.70 mmol) in toluene (20 mL) was added KOBu^t (95 mg, 0.85 mmol, 1.2 equiv). The resulting dark blue solution was stirred for 16 h, the solvent was removed under vacuum, and the dark blue residue was dissolved in hexanes (200 mL) and this solution filtered through Celite to remove solid impurities. The hexanes were removed under vacuum, and the green-black powder was washed with cold pentane (3 × 10 mL, −25 °C) to give a dark blue powder (208 mg, 0.31 mmol, 44%). This product (containing **2a** and **9a** in an 88:12 ratio) is clean by ^1H NMR, but its extreme air sensitivity has precluded satisfactory elemental analysis.

Data for **2a** are as follows. $^{31}P\{^1H\}$ NMR (202.46 MHz, δ): 276.3 (d, J_{PP} = 65 Hz, PCy_2), 63.4 (d, PPh_3). Data for **9a** are as

Table 1. 500.13 MHz ^{1}H NMR Data at 300 K[a]

	η^5-C_7H_9					
	H_7, H_4	H_6, H_5	H_2	H_3, H_1	PPh_3	other
1b[b]	7.55 (d, 1H, 9) 6.37 (d, 1H, 8)	7.38 (t, 1H, 7) 6.91 (t, 1H, 7)	5.34−5.33 (m, 1H)	4.14 (s, 1H) 3.52 (s, 1H)	7.29−7.24 (om, 9H, $H_{m,p}$) 7.03 (br s, 6H, 69, H_o)	$HPPr^i_2$: 4.16 (dt, 1H, 351, 4, P*H*), 2.59 (d octet, 1H, 4, 7, C*H*), 1.95 (d octet, 1H, 1, 8, C*H*), 1.26 (dd, 3H, 15, 7, CH_3), 1.23 (dd, 3H, 15, 7, CH_3), 1.14 (dd, 3H, 15, 8, CH_3), 0.83 (dd, 3H, 13, 8, CH_3)
1d[b]	7.54−7.50 (m, 3H, overlaps H_o (Tol^p)) 6.43 (dd, 1H, 9, 1)	7.32 (t, 1H, 7) 6.91 (t, 1H, 7)	5.04 (t, 1H, 5)	4.75−4.76 (m, 1H) 3.34 (s, 1H)	7.30−7.24 (m, 3H, H_p) 7.15−7.13 (m, 6H, H_m) 6.80 (br s, 6H, 43, H_o)	$HPTol^p_2$: 6.68 (dd, 1H, 375, 3, P*H*), 7.54−7.50 (m, 3H, overlaps H_7, H_o), 7.10−7.08 (m, 4H, H_m), 6.71−6.66 (m, 2H, H_o), 2.32 (s, 3H, CH_3) 2.43 (s, 3H, CH_3)
2a[c]	6.79−6.77 (m, 2H)	6.72−6.68 (m, 2H)	5.36 (t, 1H, 2)	5.12 (d, 2H, 2)	7.06−7.03 (om, 9H, $H_{m,p}$) 7.75−7.65 (m, 6H, H_o)	PCy_2: 2.45−2.35 (om), 1.99−1.89 (br m), 1.51−1.41 (br m), 1.25−1.15 (om), 0.42−0.32 (br m)
2b[c]	6.79−6.77 (m, 2H)	6.69−6.67 (m, 2H)	5.34 (s, 1H)	5.04 (s, 2H)	7.03 (br s, 9H, 7, $H_{m,p}$) 7.67−7.62 (m, 6H, H_o)	PPr^i_2: 2.56−2.49 (om, 1H, C*H*), 1.45 (dd, 7H, 13, 7, CH_3,C*H*), 0.51 (t, 6H, 9, CH_3)
3a[c]	7.28 (dm, 1H, 10) 5.89 (dm, 1H, 10)	6.96 (t, 1H, 10) 6.54 (t, 1H, 10)	5.91−5.90 (m, 1H)	5.29 (m, 1H) 4.90−1.89 (m, 1H)	7.03−6.98 (om, 9H, $H_{m,p}$) 7.16 (br, under solvent peak, H_o)	PCy_2: 2.38−2.36 (m), 2.22−2.14 (m), 2.08−1.98 (m), 1.86−1.84 (m), 1.75−1.72 (m), 1.63−1.40 (m), 1.35−1.15 (m), 1.01−0.93 (m)
3c[c]	7.29 (d, 1H, 9) 5.81 (d, 1H, 9)	6.99−6.92 (om, 1H, overlaps $H_{m,p}$ (PPh_3)) 6.58 (t, 1H, 8)	5.60−5.58 (m, 1H)	5.31 (s, 1H) 4.22 (s, 1H)	6.99−6.92 (om, 9H, $H_{m,p}$, overlaps H_6) 6.80 (br t, 6H, 9, H_o)	PPh_2: 7.91−7.88 (m, 2H, H_o), 7.20−7.15 (om, 5H, $H_{o,m,p}$), 7.09 (t, 2H, 8, H_m), 7.03 (t, 1H, 8, H_p)
3d[c]	7.29 (dd, 1H, 9, 1) 5.87 (dd, 1H, 9, 1)	7.02−6.9 (om, 1H, overlaps H_m ($PTol^p_2$), $H_{m,p}$ (PPh_3)) 6.60 (t, 1H, 8)	5.66−5.64 (m, 1H)	5.38−5.37 (m, 1H) 4.29−4.28 (m, 1H)	7.02−6.9 (om, 9H, $H_{m,p}$, overlaps H_m ($PTol^p_2$) and H_6) 6.84 (t, 9, H_o)	$PTol^p_2$: 7.86 (dd, 2H, 9, 5, H_o), 7.16−7.14 (m, 2H, H_o), 7.03 (br d, 2H, 8, H_m), 7.02−6.9 (om, 2H, overlaps $H_{m,p}$ (PPh_3), and H_6), 2.23 (br s, 3H, 2, CH_3), 2.16 (br s, 3H, 3, CH_3)
4a[c]	7.66 (d, 1H, 9) 6.63 (d, 1H, 8)	7.19 (t, 1H, 8) 6.87 (t, 1H, 7)	5.12−5.11 (m, 1H)	5.22 (s, 1H) 4.04 (s, 1H)	7.04 (br s, 9H, 25, $H_{m,p}$) 7.57 (br in baseline, H_o)	$PMeCy_2$: 2.54−2.48 (m), 2.05−1.92 (m), 1.80−1.79 (m), 1.73−1.69 (m), 1.62−1.58 (m), 1.50−0.93 (m), 0.93 (d, 3H, 10, PCH_3)
5a·NH$_3$[d]	7.60 (d, 1H, 8) 6.52 (dd, 1H, 8, 1)	7.52−7.46 (om, 4H, overlaps H_p) 7.14 (t, 1H, 8)	4.20 (s, 1H)	5.28 (q, 1H, 3) 5.23−5.21 (m, 1H)	7.43−7.40 (m, 6H, H_m) 7.52−7.46 (om, 4H, H_p, overlaps H_6) 6.78 (br s, 6H, 26, H_o)	$HPCy_2$: 3.91 (ddd, 1H, 325, 6, 3, P*H*). 2.12−2.05 (m), 1.99−1.90 (m), 1.81−1.79 (m), 1.72−1.71 (m), 1.61−1.50 (m), 1.43−0.98 (m), 0.84−0.75 (m) NH_3: 1.65 (br s, 3H, 9)
6a[c,e]			4.91 (s, 1H)	5.25 (s, 1H) 5.190 (s, 1H)	7.92 (t, 2H, 9, H_o) 7.44−7.34 (m), 7.26−7.00 (m), 6.93−6.86 (m)	$HPCy_2$: 3.84 (dm, 1H, 317, P*H*), 1.75−1.37 (m), 1.24−0.75 (m), 0.51−0.47 (m)
8a[b]	7.37 (d, 1H, 10) 6.16 (d, 1H, 5)	6.84 (t, 1H, 10) 7.04 (t, 1H, 5)	5.70 (s, 1H)	5.02 (s, 1H) 4.31 (s, 1H)	7.22−7.20 (br om, 9H, $H_{m,p}$) 7.50−6.50 (br in baseline, H_o)	$HPCy_2$: 4.42 (dd, 1H, 375, 5, P*H*), 2.38−2.36 (m), 2.03−2.00 (m), 1.93−1.90 (m), 1.87−1.83 (m), 1.73−1.66 (m), 1.62−1.57 (m), 1.45−1.1 (m), 1.02−0.94 (m), 0.72−0.52 (m) $SiEt_3$: 0.88 (t, 9H, 8, CH_3), 0.72−0.52 (m, 3H, CH_2), 0.44−0.36 (m, 3H, CH_2)
9a[c]	6.97 (d, 1H, 8) 6.67 (d, 1H, 8)	7.34 (t, 1H, 8) 6.92 (t, 1H, 8)	5.66 (s, 1H)[e]	4.54 (s, 1H)[f]	7.45−7.42 (m, 6H, H_o)	Ru−*H*: −15.89 (dd, 1H, 35, 33) all other peaks under signals for **2a**
9b[c]			5.63 (s, 1H)	5.12 (s, 1H) 4.56 (s, 1H)	7.43−7.39 (m, 6H, H_o)	P=C(CH_3)$_2$(^{i}Pr): 2.61−2.50 (om, 1H, C*H*), 1.92 (d, 3H,20, =C(CH_3)), 1.60 (d, 3H, 27, =C(CH_3)), 1.01(dd, 3H, 15, 7, CH_3), 0.67 (dd, 3H, 15, 7, CH_3) Ru−*H*: −15.86 (t, 1H, 35) all other peaks under signals for **2b**

[a] δ values are given in ppm; in parentheses are given the multiplicity, relative intensity, and J_{av} or $\omega_{1/2}$ values in Hz. om = overlapping multiplets. The indenyl numbering scheme is as follows:

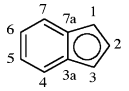

[b] Sample in $CDCl_3$. [c] Sample in C_6D_6. [d] Sample in CD_2Cl_2. [e] Unassigned indenyl protons are indistinguishable from phenyl protons. [f] Tentative assignment.

Table 2. 125.77 MHz $^{13}C\{^1H\}$ NMR Data at 300 K[a]

	η^5-C_9H_7							
	C_6, C_5	C_7, C_4	C_{3a},C_{7a}	$\Delta\delta$ ($C_{3a,7a}$)[b]	C_2	C_3, C_1	PPh_3	other
1b[c]	127.1 (s) 127.0 (s)	124.8 (s) 123.9 (s)	110.7 (d, 5) 108.8 (d, 4)	−21.0 (av)	84.1 (s)	65.6 (d, 11) 61.2 (s)	C_i (br, under C_o), 134.2 (br, 5, C_o), 129.4 (s, C_p), 127.7 (d, 9, C_m)	HP^iPr_2: 30.4 (d, 26, P*C*H), 26.8 (dd, 25, 3, P*C*H), 23.2 (d, 5, *C*H_3), 23.1 (s, *C*H_3), 22.2 (s, *C*H_3), 19.0 (s, *C*H_3)
1d[c]	127.1 (s) 126.9 (s)	124.8 (s) 123.8 (s)	111.4 (d, 4) 109.0 (d, 4)	−20.9 (av)	87.8 (s)	68.8 (d, 11) 62.0 (s)	C_i (br, under C_o), 134.0 (br, 47, C_o), 129.3 (s, C_p), 127.6 (d, 10, C_m)	$HPTol^p_2$: 140.3 (d, 4, C_p), 139.6 (d, 4, C_p), 131.7 (dd, 35, 5, C_i), 131.2(d, 40, C_i), 133.0 (d, 9, C_o), 132.7 (d, 9, C_o), 129.3 (d, 9, C_m), 128.9 (d, 11, C_m), 21.7 (s, *C*H_3), 21.6 (s, *C*H_3)
2a[d]	125.7 (s)	122.7 (s)	99.6 (s)	−31.1	76.3 (s)	66.1 (s)	141.6 (d, 36, C_i), 135.8 (d, 13, C_o), 129.7 (s, C_p), 127.7 (d, 9, C_m)	PCy_2: 50.8 (d, 7, P*C*H), 46.1 (s, P*C*H) others: 32.3 (s), 32.1 (s), 27.9−27.7 (om), 27.0−26.9 (om), 26.4 (s), 23.4 (s), 14.7 (s)
2b[d]	125.6 (s)	122.8 (s)	99.8 (s)	−30.9	76.4 (d, 5)	65.9 (s)	141.6 (d, 38, C_i) 135.9 (d, 13, C_o), 129.3 (s, C_p), 127.7 (d, 10, C_m)	P^iPr_2: 39.62 (s, P*C*H), 34.0 (s, P*C*H), 22.8 (s, *C*H_3), 17.4 (d, 10, *C*H_3)
3a[d]	126.2 (s) 124.7 (s)	122.9 (s) 121.6 (s)	113.7 (s) 110.9 (s)	−18.4 (av)	99.8 (s)	79.3 (s) 71.7 (d, 7)	135.3 (d, 42, C_i), 134.6 (dd, 11, 3, C_o), 130.1 (s, C_p), 128.2 (d, 10, C_m)	PCy_2: 42.1 (d, 44, P*C*H), 39.0 (dd, 43, 4, P*C*H) others: 37.3 (d, 29), 35.1 (d, 19), 34.0 (d, 19), 30.95 (s), 29.6 (s), 29.4 (d, 15), 28.9 (d, 9), 28.3 (d, 9), 27.5 (d, 18) CO: 205.9 (dd, 17, 12)
3c[d]	126.5 (s) 125.3 (s)	123.7 (s) 122.2 (s)	114.5 (s) 110.3 (s)	−18.3 (av)	104.3 (s)	79.7 (s) 73.6 (d, 9)	134.8 (d, 45, C_i), 134.7 (d, 10 C_o), 130.2 (d, 1, C_p), 128.2 (d, 9, C_m)	PPh_2: 152.7 (dd, 45, 5, C_i), 148.4 (d, 50, C_i), 136.3 (d, 23, C_o), 133.1 (d, 18, C_o), 128.6 (s, C_m), 128.3 (s, C_m), 127.9 (s, C_p), 125.5 (s, C_p) CO: 205.8 (dd, 16, 10)
3d[d]	126.4 (s) 125.2 (s)	123.7 (s) 122.1 (s)	114.8 (s) 110.4 (s)	−18.1 (av)	104.8 (s)	79.8 (s) 73.6 (d, 8)	134.9 (d, 58, C_i), 134.8 (d, 11, C_o), 130.2 (d, 1, C_p), 128.2 (d, 10, C_m)	$PTol^p_2$: 149.0 (dd, 45, 5, C_i), 145.0 (d, 48, C_i), 137.4 (s, C_p), 136.3 (d, 23, C_o), 133.3 (d, 18, C_o), 129.1 (os, C_m), 128.7 (s, C_p), 21.7 (s, *C*H_3), 21.6 (s, *C*H_3) CO: 206.0 (dd, 18, 16)
4a[d]	128.0 (s) 127.3 (s)	127.0 (s) 125.3 (s)	111.0 (d, 4) 108.3 (s)	−21.1 (av)	86.4 (s)	66.7 (s) 65.0 (d, 10)	135.2 (br, C_i), 129.7 (s, C_p), 128.9 (C_o, under solvent peak), 127.8 (d, 8, C_m)	$PMeCy_2$: 45.3 (dd, 23, 3, P*C*H), 42.7 (d, 23, P*C*H), 10.3 (d, 26, P*C*H_3) others (Cy): 31.65 (s), 30.8 (d, 6), 29.9 (d, 6), 28.3−29.1 (m), 27.9 (d, 8), 27.1 (d, 11)
5a·NH$_3$[e]	129.1 (s) 128.3 (s)	124.9 (s) 123.9 (s)	109.7 (d, 4) 109.0 (d, 4)	−21.4 (av)	64.5 (s)	86.4 (s) 62.7 (d, 9)	C_i (br, under C_o), 133.8 (d, 19, C_o), 131.2 (d, 1, C_p), 129.4 (d, 9, C_m)	$HPCy_2$: 42.2 (dd, 30, 2, P*C*H), 36.6 (dd, 25, 2, P*C*H) others: 34.4 (d, 9), 33.8 (d, 4), 31.6 (s), 28.2−28.0 (om), 27.7−27.5 (om), 26.3 (s)
6a[d]	123.7 (s) 122.8 (s)	122.5 (s) 121.9 (s)	109.2 (s) 107.0 (s)	−22.6 (av)	94.6 (s)	70.4 (d, 10) 63.8 (d, 10)	163.6 (dd, 24, 15, C_{o-Ru}), 152.9 (d, 47, C_i), 140.5 (d, 19, C_o), 140.0 (d, 36, C_i), 136.2 (d, 24, C_i), others: 132.8 (d, 10), 132.6 (d, 11), 129.4 (d, 3), 129.1 (s), 128.7 (s), 128.5−128.4 (m), 126.2 (s), 121.3 (d, 9)	$HPCy_2$: 36.8 (d, 23, P*C*H), 36.2 (dd, 25, 5, P*C*H) others: 32.1−31.8 (m), 31.5 (s), 28.5 (d, 13), 28.2 (d, 10), 28.1 (d, 9), 28.0 (d, 11), 27.0 (d, 9)
8a[c]	124.7 (s) 122.3 (s)	123.3 (s) 120.9 (s)	116.3 (s) 113.3 (s)	−15.9 (av)	92.1 (s)	72.9 (d, 9) 63.3 (d,10)	133.9 (br s, 36, C_i), C_o (br, in baseline), 128.6 (s, C_p), 127.3 (d, 9, C_m)	$HPCy_2$: 43.9 (dd, 24, 4, P*C*H), 41.3 (d, 18, P*C*H) others: 39.7 (d, 8), 36.1 (d, 8), 29.8 (s), 28.9 (s), 28.8 (d, 8), 28.2 (d, 11), 28.0 (d, 8), 27.2 (d, 11), 26.7 (s), 26.3 (s) $SiEt_3$: 12.5 (s, *C*H_2), 11.4 (s, *C*H_3)
9a[d,f]	123.8 (s) 123.2 (s)	122.7 (s) 122.6 (s)	110.7 (s) 108.9 (s)	−20.9 (av)	85.5 (s)	72.2 (d, 11) 66.5 (d, 9)	142.1 (d, 39, C_i), 134.5 (d, 11, C_o)	P═C(CH_2)$_5$(Cy): 37.1 (d, 16), 36.4 (d, 11), 34.78 (s), 32.7 (s), 30.6 (s), 29.8 (d, 13), 27.6 (d, 10), 26.56 (s)
9b[d,f]	124.0 (s) 123.3 (s)	122.7 (s) 122.6 (s)	110.7 (s) 108.5 (s)	−21.1 (av)	85.2 (s)	72.1 (d, 9) 66.6 (d, 9)	141.9 (d, 34, C_i), 134.4 (d, 11, C_o), 129.0 (s, C_p)	P═C(CH_3)$_2$(^{i}Pr): 22.5 (s, ═C(CH_3)), 20.5 (s, ═C(CH_3)) others: 31.3 (d, 9), 27.2 (d, 13), 25.2 (d, 10)

[a] δ values are given in ppm; in parentheses are given the multiplicity and J_{PC} or $\omega_{1/2}$ values in Hz. om = overlapping multiplets. See footnote *a* in Table 1 for the indenyl numbering scheme. [b] $\Delta\delta(C_{3a,7a}) = \delta(C_{3a,7a}(\eta\text{-indenyl complex})) - \delta(C_{3a,7a}(\eta\text{-sodium indenyl}))$. $\delta(C_{3a,7a})$ for sodium indenyl is 130.7 ppm.[22] [c] Sample in $CDCl_3$. [d] Sample in C_6D_6. [e] Sample in CD_2Cl_2. [f] Due to the small abundance of complexes **9a** (12%) and **9b** (16%), not all of their ^{13}C peaks could be assigned.

Table 3. Crystallographic Data

	2a·0.25(pentane)	**3a**	**[5a·NH$_3$]PF$_6$**	**8a**
formula	$C_{40.25}H_{47}P_2Ru$	$C_{40}H_{44}OP_2Ru$	$C_{39}H_{48}F_6NP_3Ru$	$C_{45}H_{60}P_2RuSi$
formula wt	693.79	703.76	838.76	792.03
cryst growth conditions	slow evap from min vol of pentane	min vol of toluene with layered pentane (1:8 vol ratio)	min vol of CH_2Cl_2 with slow vapor diffusion of diethyl ether (1:5 vol ratio)	min vol of toluene with layered pentane (1:10 vol ratio)
cryst color	purple	orange	orange	yellow
cryst dimens (mm)	0.46 × 0.18 × 0.13	0.55 × 0.18 × 0.09	0.64 × 0.17 × 0.16	0.42 × 0.23 × 0.17
cryst syst, space group	monoclinic, $P2_1/n$	triclinic, $P\bar{1}$	triclinic, $P\bar{1}$	triclinic, $P\bar{1}$
a (Å)	10.3907(13)	9.8311(12)	9.1385(4)	11.5039(14)
b (Å)	13.5621(16)	12.3025(15)	10.8856(5)	12.0314(14)
c (Å)	25.866(3)	15.6685(19)	20.1951(8)	16.4281(19)
α(deg)		97.7025(17)	100.9043(7)	81.4603(17)
β (deg)	100.432(2)	101.4607(17)	92.2008(7)	89.8746(17)
γ (deg)		110.8896(16)	107.7646(6)	64.4406(15)
V (Å^3)	3584.8(8)	1691.2(4)	1868.68(14)	2023.6(4)
Z	4	2	2	2
ρ_{calcd} (g cm^{-3})	1.285	1.382	1.491	1.300
μ (mm^{-1})	0.553	0.589	0.608	0.526
total data collected	26 806 ($-12 \le h \le 12$, $-16 \le k \le 16$, $-32 \le l \le 32$)	13 520 ($-12 \le h \le 12$, $-15 \le k \le 15$, $-19 \le l \le 19$)	14 476 ($-11 \le h \le 11$, $-13 \le k \le 13$, $-25 \le l \le 25$)	15 662 ($-14 \le h \le 14$, $-14 \le k \le 14$, $-20 \le l \le 20$)
no. of indep rflns	7309 (R_{int} = 0.0956)	6929 (R_{int} = 0.0231)	7611 (R_{int} = 0.0187)	8117 (R_{int} = 0.0274)
no. of obsd rflns ($F_o^2 \ge 2\sigma(F_o^2)$)	4859	6285	6961	6661
no. of data/restraints/params	7309/0/379	6929/0/397	7611/0/456	8117/3[a]/452
goodness of fit (S)[b]	0.981	1.137	1.091	1.111
R1 ($F_o^2 \ge 2\sigma(F_o^2)$)[c]	0.0603	0.0298	0.0286	0.0315
wR2 (all data)[d]	0.1576	0.0772	0.0816	0.0860
largest diff peak, hole (e Å^{-3})	1.929, −1.062	0.501, −0.299	0.749, −0.434	0.483, −0.463

[a] Distances involving a disordered Si−Et group were constrained to be equal (within 0.001 Å) during refinement: d(Si−C65A) = d(Si−C65B); d(Si···C66A) = d(Si···C66A); d(C65A−C66A) = d(C65B−C66B). [b] $S = [\sum w(F_o^2 - F_c^2)^2/(n-p)]^{1/2}$ (n = number of data; p = number of parameters varied; $w = [\sigma^2(Fo^2) + (A_0P)^2 + A_1P]^{-1}$. A values are as follows: for **2a**, A_0 = 0.0891, A_1 = 0; for **3a**, A_0 = 0.0235, A_1 = 1.6166; for **[5a·NH$_3$]PF$_6$**, A_0 = 0.0467, A_1 = 0.7394; for **8a**, A_0 = 0.0439, A_1 = 0.2208. [c] $R1 = \sum||F_o| - |F_c||/\sum|F_o|$. [d] $wR2 = [\sum w(F_o^2 - F_c^2)^2/\sum w(F_o^4)]^{1/2}$.

follows. $^{31}P\{^1H\}$ NMR (202.46 MHz, δ): 243.4 (d, J_{PP} = 36 Hz, "*P*Cy$_2$"), 62.3 (d, *P*Ph$_3$). ^1H NMR (500 MHz, δ_{Ru-H}): −15.89 ppm. Inert-atmosphere MALDI-TOF-MS of the **2a/9a** mixture (pyrene in benzene matrix; *m*/*z* (relative intensity)): 676.6 (100%) [M$^+$], 479.6 (33%) [M$^+$ − PCy$_2$], 412.6 (10%) [M$^+$ − PPh$_3$].

Method B. This alternate method allows the synthesis of (slightly less pure) **2a** on a scale larger than that given above. To a Schlenk flask containing a dark red solution/suspension of **1a** (736 mg, 1.0 mmol) in toluene (20 mL) was added KOBu^t (134 mg, 1.2 mmol, 1.2 equiv). The resulting dark blue solution was stirred for 16 h before the solvent was removed by evaporation to give a dark blue oil. The product was redissolved in a 1:5 toluene/hexanes solution (2 × 25 mL) and filtered through Celite to remove any solid impurities. The solvent was removed under vacuum, and the green-black powder was washed with cold pentane (3 × 10 mL, −30 °C), resulting in a dark blue powder (545 mg, 0.81 mmol, 81% crude yield).

(b) [Ru(PPr$^i_2$)(η^5-indenyl)(PPh$_3$)] (2b). To a dark red solution/suspension of **1b** (75 mg, 0.12 mmol) in toluene (5 mL) was added KOBu^t (16 mg, 0.14 mmol, 1.2 equiv). The resulting dark blue solution was stirred for 2 h to ensure complete reaction, the solvent was removed under vacuum, the resulting dark blue oil was dissolved in pentane (5 mL), and this solution was filtered through Celite to remove solid impurities. The solution was placed in the freezer (−30 °C) for 3 days, and dark blue crystals (61 mg, 0.10 mmol, 83%) were isolated after filtration and 3 × 10 mL washings with cold pentane (−30 °C). ^1H NMR shows this product (containing **2b** and **9b** in an 84:16 ratio) contains ∼0.5 equiv of pentane but is otherwise clean. Its extreme air sensitivity, however, has precluded elemental analysis.

Data for **2b** are as follows. $^{31}P\{^1H\}$ NMR (202.46 MHz, C_6D_6, δ): 288.3 (d, J_{PP} = 65 Hz, *P*^{i}Pr$_2$), 63.2 (d, *P*Ph$_3$). Data for **9b** are as follows. $^{31}P\{^1H\}$ NMR (202.46 MHz, C_6D_6, δ): 256.4 (d, J_{PP} = 38 Hz, "*P*^{i}Pr$_2$"), 63.2 (d, *P*Ph$_3$, overlapping with signal due to **2b**). Over time, the ortho-metalated product **6b** was also observed in solutions of **2b/9b**. Data for **6b** are as follows. $^{31}P\{^1H\}$ NMR (145.80 MHz, C_6D_6, δ): 66.5 (d, J_{PP} = 29 Hz, H*P*Cy$_2$), −20.8 (d, *P*Ph$_3$).

(c) [Ru(PCy$_2$)(η^5-indenyl)(CO)(PPh$_3$)] (3a). A Schlenk flask containing a dark blue solution of **2a** (160 mg, 0.24 mmol) in toluene (2 mL) was placed under an atmosphere of CO. The resulting dark red solution was stirred for 10 min before the solvent was removed under vacuum. Addition of pentane (5 mL) to the residue gave an orange-red suspension, which was filtered and washed with cold pentane (3 × 5 mL) to give an orange-red powder (120 mg, 0.17 mmol, 71% crude yield). Recrystallization from toluene (5 mL) by slow diffusion of a layer of pentane (40 mL) gave [Ru(PCy$_2$)(η^5-indenyl)(CO)(PPh$_3$)] (**3a**) as a red crystalline solid (54 mg, 0.08 mmol, 45% yield). $^{31}P\{^1H\}$ NMR (202.46 MHz, C_6D_6, δ): 56.9 (d, $^2J_{PP}$ = 8 Hz, *P*Cy$_2$), 52.2 (d, *P*Ph$_3$). IR (KBr, cm^{-1}); 1931 (s, ν_{CO}). FAB-MS (+LSIMS matrix mNBA; *m*/*z* (relative intensity)): 705.2 (100%) [M$^+$ + H], 479.0 (27%) [M$^+$ − HPCy$_2$ − CO]. HR-MS (+LSIMS matrix mNBA): exact mass (monoisotopic) calcd for $C_{40}H_{44}OP_2Ru$ + H, 705.1989; found, 705.1983 ± 0.0035 (average of 3 trials). Anal. Calcd for $C_{40}H_{44}OP_2Ru$: C, 68.26; H, 6.30. Found: C, 68.17; H, 6.55. Dec pt: 161−163 °C.

(d) [Ru(PPh$_2$)(η^5-indenyl)(CO)(PPh$_3$)] (3c). In a Schlenk flask containing **1c** (299 mg, 0.43 mmol), a dark red solution/suspension was formed by addition of toluene (5 mL). The solution was saturated with CO, and then KOBu^t (96 mg, 0.86 mmol, 2 equiv) was added. The resulting dark red solution was stirred for 10 min, and then solvent and excess CO were removed under vacuum to give a purple solid. A solution of the residue in toluene (30 mL) was filtered through Celite to remove solid impurities and then concentrated to 5 mL under vacuum. Recrystallization by slow layer diffusion of pentane (40 mL) at low temperature (−30 °C) gave dark purple crystals of [Ru(PPh$_2$)(η^5-indenyl)(CO)(PPh$_3$)] (**3c**; 241 mg, 0.35 mmol, 81%). $^{31}P\{^1H\}$ NMR (202.46 MHz, C_6D_6, δ): 51.7 (d, $^2J_{PP}$ = 8 Hz, *P*Ph$_3$), 17.9 (d, *P*Ph$_2$). IR (KBr, cm^{-1}); 1921 (s,

ν_{CO}). FAB-MS (+LSIMS matrix mNBA; *m*/*z* (relative intensity)): 693.0 (100%) [$M^+ + H$], 506.9 (17%) [$M^+ - HPPh_2$], 478.9 (58%) [$M^+ - HPPh_2 - CO$], 401.9 (18%) [$M^+ - PPh_3 - CO$]. HR-MS (+LSIMS matrix mNBA): exact mass (monoisotopic) calcd for $C_{40}H_{32}OP_2Ru + H$, 693.1050; found, 693.1071 ± 0.0038 (average of 3 trials). Anal. Calcd for $C_{40}H_{32}OP_2Ru$: C, 69.46; H, 4.66. Found: C, 69.41; H, 4.68. Dec pt: 163−166 °C.

(e) [Ru(PTol$^p_2$)(η^5-indenyl)(CO)(PPh$_3$)] (3d). In a Schlenk flask containing **1d** (254 mg, 0.35 mmol) a dark red solution/suspension was formed by addition of toluene (5 mL). The solution was saturated with CO, and then KOBu^t (78 mg, 0.70 mmol, 2 equiv) was added. The resulting dark red solution was stirred for 10 min before solvent and excess CO were removed under vacuum to give a strawberry red solid. The product was redissolved in toluene (30 mL) and this solution filtered through Celite to remove solid impurities. The solution was reduced to 2 mL under vacuum and recrystallized by slow layer diffusion of pentane (50 mL) at low temperature (−30 °C) to give [Ru(PTol$^p_2$)(η^5-indenyl)(CO)(PPh$_3$)] (**3d**) as a red crystalline solid (175 mg, 0.24 mmol, 69%). $^{31}P\{^1H\}$ NMR (202.46 MHz, C_6D_6, δ): 51.8 (d, $^2J_{PP}$ = 7 Hz, *P*Ph$_3$), 17.3 (d, *P*Tol$^p_2$). IR (KBr, cm^{-1}): 1926 (s, ν_{CO}). FAB-MS (+LSIMS matrix mNBA; *m*/*z* (relative intensity)): 721.1 (100%) [$M^+ + H$], 478.9 (65%) [$M^+ - HPTol^p_2 - CO$], 430.9 (21%) [$M^+ - PPh_3 - CO$]. HR-MS (+LSIMS matrix mNBA): exact mass (monoisotopic) calcd for $C_{42}H_{36}OP_2Ru + H$, 721.1363; found, 721.1361 ± 0.0031 (average of 3 trials). Anal. Calcd for $C_{42}H_{36}OP_2Ru$: C, 70.09; H, 5.04. Found: C, 69.21; H, 4.93. Dec pt: 155−156 °C. (We note that the crude product is consistently accompanied by a small amount (≤5%) of [Ru(PTol$^p_2$)(η^5-indenyl)(CO)$_2$], resulting from substitution of PPh$_3$ ($^{31}P\{^1H\}$ NMR (202.46 MHz, C_6D_6, δ): 63.8 (s, *P*Tol$^p_2$)), even with very short reaction times.)

(f) [Ru(η^5-indenyl)I(PMeCy$_2$)(PPh$_3$)] (4a). To a Schlenk flask containing a dark blue solution of **2a** (220 mg, 0.32 mmol) in toluene (2 mL) was added MeI (0.10 mL, 1.6 mmol, excess). The reaction mixture was stirred for 1 h, to give a dark red solution. The solvent was removed under vacuum, and pentane (5 mL) was added to give a red-brown suspension, which was filtered and washed with cold pentane (3 × 5 mL) to give [Ru(η^5-indenyl)I(PMeCy$_2$)(PPh$_3$)] (**4a**; 197 mg, 0.24 mmol, 75% crude yield). A crude sample (102 mg, 0.12 mmol) was recrystallized from benzene (5 mL) by slow vapor diffusion of hexanes to give analytically pure **4a** (82 mg, 0.10 mmol, 80%). $^{31}P\{^1H\}$ NMR (202.46 MHz, $CDCl_3$, δ): 49.5 (d, J_{PP} = 37 Hz, *P*Ph$_3$), 39.2 (d, *P*MeCy$_2$). FAB-MS (+LSIMS matrix mNBA; *m*/*z* (relative intensity)): 818.1 (36%) [M^+], 691.2 (89%) [$M^+ - I$], 605.9 (18%) [$M^+ - MePCy_2$], 556.0 (100%) [$M^+ - PPh_3$], 478.9 (68%) [$M^+ - I - MePCy_2$], 344.9 (73%) [$M^+ - PPh_3 - MePCy_2$]. HR-MS (+LSIMS matrix mNBA): calcd for $C_{40}H_{47}IP_2Ru$, 818.1241; found, 818.1255 ± 0.0018 (average of 3 trials). Anal. Calcd for $C_{40}H_{47}IP_2Ru$: C, 58.75; H, 5.79. Found: C, 58.63; H, 5.66. Dec pt: 115−116 °C.

(g) [Ru(η^5-indenyl)(NH$_3$)(HPCy$_2$)(PPh$_3$)]PF$_6$ ([5a·NH$_3$]PF$_6$). To a solution of **2a** (97 mg, 0.14 mmol) in toluene (3 mL) was added [NH_4][PF_6] (23 mg, 0.14 mmol). With stirring, the blue solution slowly (12−16 h) changed to a yellow suspension, which was filtered and washed with hexanes (3 × 5 mL) to give a bright yellow powder (108 mg). Recrystallization from CH_2Cl_2 (2 mL) by the slow vapor diffusion of ether (10 mL) gave analytically pure **[5a·NH$_3$](PF$_6$)** (69 mg, 0.082 mmol, 60%). $^{31}P\{^1H\}$ NMR (202.46 MHz, CD_2Cl_2, δ): 59.4 (d, $^2J_{PP}$ = 38 Hz, H*P*Cy$_2$), 55.0 (d, *P*Ph$_3$), −144.0 (sept, $^1J_{PF}$ = 710 Hz, PF_6^-). IR (KBr, cm^{-1}): 3354 (w, ν_{N-H}), 2342 (w, ν_{P-H}). FAB-MS (+LSIMS matrix mNBA; *m*/*z* (relative intensity)): 694.2 (13%) [M^+], 677.2 (100%) [$M^+ - NH_3$], 479.0 (31%) [$M^+ - NH_3 - HPCy_2$], 413 (15%) [$M^+ - NH_3 - PPh_3 - H^+$]. HR-MS (+LSIMS matrix mNBA): calcd for $C_{39}H_{48}NP_2Ru$, 694.2306; found, 694.2307 ± 0.0007 (average of 3 trials). Anal. Calcd for $C_{39}H_{48}F_6NP_3Ru$: C, 55.85; H, 5.77. Found: C, 55.56; H, 5.62. Dec pt: 169−171 °C.

(h) [Ru(η^5-indenyl)(SiEt$_3$)(HPCy$_2$)(PPh$_3$)] (8a). To a solution of **2a** (81 mg, 0.12 mmol) in toluene (2 mL) was added $HSiEt_3$ (14 mg, 0.12 mmol) in toluene (2 mL). With stirring, the dark blue mixture slowly changed to golden yellow (12−16 h). The solvent was removed under vacuum, and pentane (1 mL) was added to give a yellow suspension, which was filtered and washed with cold pentane (3 × 5 mL). Slow evaporation (−25 °C) of a toluene solution (5 mL) of the resulting yellow powder (42 mg) gave analytically pure **7a** (29 mg, 0.037 mmol, 31%). $^{31}P\{^1H\}$ NMR (202.46 MHz, $CDCl_3$, δ): 55.3 (d, $^2J_{PP}$ = 28 Hz, *P*Ph$_3$), 47.5 (d, H*P*Cy$_2$). IR (KBr, cm^{-1}): 2307 (w, ν_{P-H}). Anal. Calcd for $C_{45}H_{60}SiP_2Ru$: C, 68.24; H, 7.63. Found: C, 68.12; H, 7.38. Dec pt: 161−164 °C.

NMR Scale Reactions of 2a.

(a) Reaction with [HNEt$_3$][Cl]. Solid **2a** (30 mg, 0.044 mmol) and [$HNEt_3$][Cl] (6 mg, 0.04 mmol) were placed in a sealable NMR tube. CD_2Cl_2 (0.8 mL) was transferred under vacuum, and the tube was flame-sealed. The thawed solution was shaken to mix the reagents before being placed in the NMR spectrometer, where the disappearance of **2a** and appearance of **1a** was monitored by $^{31}P\{^1H\}$ NMR spectroscopy. Complete consumption of **2a** occurred within 30 min at room temperature, giving ∼90% of **1a**.

(b) Reaction with HCl. Solid **2a** (31 mg, 0.046 mmol) was placed in a sealable NMR tube, and C_6D_6 (0.8 mL) was transferred under vacuum. Ethereal HCl (2 M, 28 μL, 0.057 mmol) was added, and the tube was flame-sealed. The thawed solution was shaken for 5 min to mix the reagents before being placed in the NMR spectrometer; however, the blue color of the solution did not immediately disappear. The slow consumption of **2a** may be due to the low solubility of HCl in benzene. After 20 min the mixture contained compound **1a** (32%) along with **2a**, **9a**, and other unidentified products. After 2 days, the sample was yellow-orange and contained **1a** as the major product (66%).

(c) Thermal Decomposition. Solid **2a** (25 mg, 0.037 mmol) and triphenylphosphine oxide (13.1 mg, 0.047 mmol, internal standard) were placed in a sealable NMR tube. C_7D_8 (0.8 mL) was transferred under vacuum, and the tube was flame-sealed. The progress of the reaction was monitored at 77 °C (probe temperature) by $^{31}P\{^1H\}$ NMR. Complete consumption of **2a** (5.5 h) gave mainly [Ru(η^5-indenyl)\{κ^2-(*o*-C_6H_4)PPh_2\}(HPCy$_2$)] (**6a**; 89%).

Data for **6a** are as follows. $^{31}P\{^1H\}$ NMR (202.46 MHz, δ): 57.2 (d, J_{PP} = 28 Hz, H*P*Cy$_2$), −20.0 (d, *P*Ph$_3$).

(d) Reaction with H$_2$(g). Solid **2a** (25 mg, 0.037 mmol) and triphenylphosphine oxide (10.4 mg, 0.037 mmol, internal standard) were placed in a sealable NMR tube. C_6D_6 (0.8 mL) was transferred under vacuum, and slightly less than 1 atm of hydrogen gas was introduced before the tube was flame-sealed. The thawed solution was shaken until the dark blue solution turned yellow (5 min). $^{31}P\{^1H\}$ NMR showed the conversion of **2a** to [Ru(η^5-indenyl)(H)(HPCy$_2$)(PPh$_3$)] (**7a**) (98%).

Other NMR Scale Reactions.

(a) Monitoring the Formation of [Ru(PPh$_2$)(η^5-indenyl)(PPh$_3$)] (2c). Toluene-d_8 (0.8 mL) was transferred under vacuum to a sealable NMR tube containing solid **1c** (26 mg, 0.037 mmol) and KOBu^t (5 mg, 0.044 mmol, 1.2 equiv), frozen in N_2(l). The tube was flame-sealed and placed in an acetone/dry ice bath to thaw. The sample was then placed in the 360 MHz NMR spectrometer precooled to 230 K, and the progress of the reaction was monitored by $^{31}P\{^1H\}$ NMR spectroscopy as the temperature was increased in 5 K intervals. At 245 K a small amount of [Ru(PPh$_2$)(η^5-indenyl)(PPh$_3$)] (**2c**; ∼25%) was observed, but no further change occurred as the temperature was increased to 260 K. The sample (a green solution) was removed, quickly shaken, and then placed back in the spectrometer. The main product was still unreacted **1c** (∼40%) with an unchanged amount of **2c** (∼25%) and other, unidentified products (∼35%). The sample was then removed from the spectrometer and warmed. When it reached room temperature, the

dark green solution spontaneously turned black, giving a complex mixture of unidentified products.

Data for **2c** in C_7D_8 at 250 K are as follows. $^{31}P\{^1H\}$ NMR (145.80 MHz, δ): 195.8 (d, $J_{PP} = 63$ Hz, $P\text{Ph}_2$), 58.2 (d, $P\text{Ph}_3$).

(b) Monitoring the Formation of [Ru(PTol$^p_2$)(η^5-indenyl)(PPh$_3$)] (2d). Toluene-d_8 (0.8 mL) was transferred under vacuum to a sealable NMR tube containing solid **1d** (28 mg, 0.038 mmol) and KOBu^t (5 mg, 0.046 mmol, 1.2 equiv), frozen in N_2(l). The tube was flame-sealed and placed in an acetone/dry ice bath to thaw. The sample was then placed in the 360 MHz NMR spectrometer precooled to 190 K. The progress of the reaction was monitored by $^{31}P\{^1H\}$ NMR spectroscopy as the temperature was increased in 5 K intervals. At 250 K a small singlet appeared at 66.2 ppm. No new product formation was observed as the temperature was increased to 260 K. The sample was removed from the spectrometer, shaken quickly, resulting in a green solution, and then placed back in the spectrometer. The main product was still the unknown complex at 66.2 ppm (~40%), but [Ru(P(Tol^p)$_2$)(η^5-indenyl)(PPh$_3$)] (**2d**, ~36%) and other unidentified products (~24%) were also observed. At room temperature the green color of this mixture persisted for ~1 h, before decomposing to a black mixture of unidentified products.

Data for **2d** in C_7D_8 at 260 K are as follows. $^{31}P\{^1H\}$ NMR (145.80 MHz, δ): 201.7 (d, $J_{PP} = 63$ Hz, $P\text{Tol}^p_2$), 60.6 (d, $P\text{Ph}_3$).

Crystallographic Study of 2a. Attempts to refine peaks of residual electron density as solvent *n*-pentane carbon atoms in crystals of **2a** were unsuccessful. The data were corrected for disordered electron density through use of the SQUEEZE procedure[23] as implemented in PLATON.[24] A total solvent-accessible void volume of 521.7 Å^3 with a total electron count of 91 (consistent with one molecule of solvent *n*-pentane) was found in the unit cell.

Computational Details. Geometry optimization and time-dependent (TD-DFT) calculations were performed with the hybrid PBE1PBE density functional, which incorporates 25% of exact exchange.[25] The relativistic effective core potential of the Stuttgart group (ECP28MWB) along with the associated valence basis set were used for ruthenium.[26] In the calculations of the simplified models of **2**/**9** and their interconversion the 6-31++G(d,p) basis sets were used for P, C, and H, whereas calculations on **2a** with the full ligand system employed the 6-31G(d) basis sets for phosphorus and the indenyl carbons and the STO-3G basis sets for the remaining atomic centers. All calculations were performed with Gaussian03,[27] and the TD-DFT results were analyzed with the SWizard program.[28] Ellipticity values were determined from analysis of the electron density with XAim.[29]

Acknowledgment. We thank the NSERC of Canada for financial support, Prof. John E. McGrady (University of Glasgow) for helpful discussions, Prof. Deryn E. Fogg and Johanna M. Blacquiere (University of Ottawa) for inert-atmosphere MALDI-TOF analysis, and Shaun A. Hall (University of Victoria) for the preparation of complex **1d**.

Supporting Information Available: Tables giving DFT optimized coordinates and calculated energies and CIF files giving crystallographic data. This material is available free of charge via the Internet at http://pubs.acs.org.

OM0700056

(22) Gamasa, M. P.; Gimeno, J.; Gonzalez-Bernardo, C.; Martin-Vaca, B. M. *Organometallics* **1996**, *15*, 302.

(23) van der Sluis, P.; Spek, A. L. *Acta Crystallogr.* **1990**, *A46*, 194.

(24) Spek, A. L. *Acta Crystallogr.* **1990**, *A46*, C34 (PLATON-A Multipurpose Crystallographic Tool; Utrecht University, Utrecht, The Netherlands).

(25) Perdew, J. P.; Burke, K.; Ernzerhof, M. *Phys. Rev. Lett.* **1996**, *77*, 3865.

(26) Andrae, D.; Haussermann, U.; Dolg, M.; Stoll, H.; Preuss, H. *Theor. Chim. Acta* **1990**, *77*, 123.

(27) Frisch, M. J., et al. *Gaussian 03* (Revision B.03); see the Supporting Information.

(28) Gorelsky, S. I. SWizard program; http://www.sg-chem.net.

(29) Ortiz Alba, J. C.; Bo, C. Xaim-1.0; Universitat Rovira i Virgili, Tarragona, Spain.